Biometals (2017) 30:893–902
DOI 10.1007/s10534-017-0055-5

Biocidal properties of maltose reduced silver nanoparticles against American foulbrood diseases pathogens

Mustafa Çulha · Şaban Kalay · Elif Sevim · Müberra Pinarbaş · Yıldız Baş · Rahşan Akpinar · Şengül Alpay Karaoğlu

Received: 31 August 2017 / Accepted: 29 September 2017 / Published online: 6 October 2017

Abstract Bee disease caused by spore-forming *Paenibacillus larvae* and *Paenibacillus alvei* is a serious problem for honey production. Thus, there is an ongoing effort to find an effective agent that shows broad biocidal activity with minimal environmental hazard. In this study, the biocidal effect of maltose reduced silver nanoparticles (AgNPs) is evaluated against American foulbrood and European foulbrood pathogens. The results demonstrate that the maltose reduced AgNPs are excellent short and long-term biocides against *P. larvae* isolates. The long-term effect suggests that the Ag^{+} ions are released from the AgNPs with increasing time in a controlled manner.

M. Çulha (✉) · Ş. Kalay
Department of Genetics and Bioengineering, Yeditepe University, Atasehir, 34755 Istanbul, Turkey
e-mail: mculha@yeditepe.edu.tr

E. Sevim
Genetics and Bioengineering Department, Faculty of Engineering and Architecture, Ahievran University, Kırşehir, Turkey

M. Pinarbaş · Y. Baş · Ş. A. Karaoğlu
Department of Biology, Faculty of Arts & Sciences, Recep Tayyip Erdoğan University, Rize, Turkey

R. Akpinar
Bee Hospital Laboratory, Veterinary Control Institute, Samsun, Turkey

Keywords Silver nanoparticles · Honeybee pathogens · American foulbrood · European foulbrood · AgNPs

Introduction

The fight against pathogenic microorganisms is always a fierce battle to prevent their destructive effects. Among many biocides, there is an increasing interest to use colloidal silver nanoparticles (AgNPs) due to their broad spectrum of biocidal effect, low cost and relatively simple synthesis (Biswas et al. 2012; Brust and Kiely 2002; Dong et al. 2009; Vahabi et al. 2011). AgNPs included in various consumer products such as shampoos, cosmetics and composite materials (Dubas et al. 2006; Frey et al. 2009; Haider and Kang 2015; Kong and Jang 2008; Petros and DeSimone 2010; Tugulea et al. 2014). In addition, AgNPs have other unique properties such as plasmonic and high electrical and thermal conductivity, which make them attractive nanomaterials for their use in a range of applications including chemo and biosensors, conductive inks, pigments and substrates in surface-enhanced Raman scattering (Besinis et al. 2014; Lee and Meisel 1982; Sharma et al. 2009; Tran et al. 2013). The antimicrobial activity of colloidal AgNPs were thoroughly investigated in recent years and their biocidal activity against a number of highly pathogenic and drug-resistant Gram− and Gram+ bacteria including

Klebsiella pneumoniae, Pseudomonas aeruginosa, Bacillus cereus, Enterococcus fecalis, Micrococus luteus, vancomycin resistant enterococci was demonstrated (Besinis et al. 2014; Kong and Jang 2008; Morones et al. 2005; Sharma et al. 2009).

AgNPs are easily synthesized with aqueous synthesis methods in which silver ions from one of its salts are reduced with a reducing agent. Many reducing agents such as hydrazine, borohydride, citrate, ascorbic acid, starch, monosaccharides, disaccharides and Tollens reagent have been reported (Dong et al. 2009; Haider and Kang 2015; Lee and Meisel 1982; Mochochoko et al. 2013; Sharma et al. 2009; Tran et al. 2013; Vahabi et al. 2011). Some of the reducing agents are claimed to be environmental friendly since they are either a biomolecule or a plant extract (Mochochoko et al. 2013; Sharma et al. 2009; Vahabi et al. 2011). For example, glucose was used as a reducing agent to synthesize AgNP average size 10 nm in a mildly heated environment less than 10 min (Raveendran et al. 2003; Sharma et al. 2009). During AgNP synthesis, starch was added as capping agent to stabilize the AgNPs. In another example, the disaccharide maltose was used as a reducing agent for the AgNP synthesis with the assistance of microwave radiation. Polyvinylpyrrolidone was added into the reaction mixture to stabilize the formed AgNPs (Singh et al. 2014). An anisotropic mixture of AgNPs with an average size of 39 nm was obtained.

The size and dissolution rate of AgNPs determine the overall biocidal activity of AgNPs. Smaller sizes of AgNPs show higher biocidal activity since the AgNPs in the range of 1–10 nm adhere to bacterial cell membranes and dramatically disrupt its function (Ansari et al. 2015). The AgNPs with a few nanometers can also pass across bacterial walls and can bind to DNA and proteins in the bacterial cell. The other factor is the dissolution rate of the AgNPs (release Ag^+ cations) and a higher dissolution rate with reduced size is reported (Dobias and Bernier-Latmani 2013). The biocidal activity of Ag^+ ions is widely known (Agnihotri et al. 2014; Ansari et al. 2015; Kong and Jang 2008; Morones et al. 2005; Pal et al. 2007; Tran et al. 2013). AgNPs behave as slow Ag^+ ion releasing units (Dobias and Bernier-Latmani 2013; Morones et al. 2005; Pal et al. 2007). The ion releasing behavior not only depends on size but also synthesis method. The shape of the AgNPs is also reported to be an important factor for their biocidal effect (Pal et al. 2007). Triangular shaped AgNPs with a (111) lattice were found to be more effective against *Escherichia coli* as compared to the spherical ones (Pal et al. 2007).

Spore-forming *Paenibacillus* are almost ubiquitous in nature including soil, water, vegetable matter and insect larvae, and some of these strains are pathogens. American foulbrood diseases caused by larvae is most serious disease for honey bees (*Apis mellifera*). *P. larvae is* a Gram-positive spore-forming bacterium (Genersch 2010; Özkırım et al. 2015). Although *P. larvae* does not affect adult bees, it is very infectious for larva (Wilson 1971). The spores are resistant to heat and chemical agents and can survive for many years in hive products and equipment (OIE, World Organisation of Animal Health,Terrestrial Manual. Ch. 2.2.2. 2017). Similar to American foulbrood disease, the other major contagious disease is European foulbrood caused by *Melisococcus plutonius* as primary pathogen and *Paenibacillus alvei, Bacillus laterosporus, Enterococcus faecalis, Acromobacter euridice, Brevibacillus laterosporus* as secondary pathogens (Chauzat and Laddomada 2015).

A number of available antibiotics including sulfonamids, oxytetracycline, streptomycin, tylosin, and erythromycin have been used for the treatment of American foulbrood and European foulbrood (Reybroeck et al. 2012). However, the use of antibiotics is not safe since they have adverse effects on environment and human health. Long term antibiotic use has the risk of developing resistance and further complicating the battle against the disease (Llror and Bjerrum 2014). Therefore, there is an effort to find alternative strategies to antibiotic use in recent years.

In this study, AgNPs were synthesized using a green-chemistry approach, which involves the reduction of Ag^+ ions with maltose monohydrate without using a stabilizer, as different from the previously reported studies. The obtained AgNPs were characterized with transmission electron microscopy and spectroscopic techniques such as UV–vis, fourier transform infrared scectroscopy (FTIR) and dynamic light scattering (DLS). The biocidal activity of AgNPs was tested on two groups of microorganisms causing American and European foulbrood disease pathogens. The microorganisms in the first group are *P. larvae, P. alvei* and spore-forming *Bacillus* strains isolated from American and European foulbrood disease suspicious larva and honey samples. The other group microorganisms

consist of some Gram− and + bacteria chosen based on their clinical and pharmacological importance.

Materials and methods

Silver nitrate (> 99.9% pure) and absolute ethanol (≥ 99.8%) were purchased from Sigma Company (Saint Louis, USA). Maltose monohydrate (> 99.5% pure), nitric acid (≥ 65%) were obtained from Merck (Darmstadt, Germany). Deionized water (18.2 MΩ cm^{-1}) was used for all experiments.

Synthesis of silver nanoparticles

A solution prepared by dissolving 0.475 g of $AgNO_3$ in 10 mL water, which was added drop-wise into a boiling and stirring maltose monohydrate solution prepared by dissolving a 50 g maltose in 100 ml water on a hot plate. After completing the drop-wise addition of $AgNO_3$ solution, the reaction mixture was boiled for additional 15 min to obtain the AgNP colloidal suspension.

Characterization of silver nanoparticles

The optical absorption spectra of AgNPs suspension were recorded on a double-beam UV–Vis spectrophotometer Lambda 35 (Perkin Elmer, Germany) by scanning in the range of 300-900 nm at room temperature. The size distribution and zeta potential of AgNPs in its suspension was measured using a Zetasizer Nano ZS instrument (Malvern, UK) equipped with a 4-mW He–Ne laser at 173° scattering angle at room temperature.

The FTIR spectra were obtained with Nicolet IS50 FTIR (Thermo Scientific). Briefly, a 35 ml of absolute ethanol was added into a 15 ml of AgNPs colloidal suspension, vortexed and sedimented by centrifuging at 10,400×*g* (JS-7.5 rotor, 30 min, 24 °C, Beckman Avanti J-25 I). After three washing steps with ethanol, FTIR spectra were obtained from the remaining precipitate at least 3 h of drying at 70 °C.

Transmission electron microscopy

Transmission Electron Microscopy (TEM) measurements were performed with JEOL-2100 instrument operating at 120 kV (LaB6 filament) equipped with an Oxford Instruments 6498 EDS system.

Microorganisms

The first group of bacteria including *Bacillus*, *Paenibacillus* and *Micrococcus* strains were isolated from larva and honey samples confirmed as diseased in the microbiology laboratories of Recep Tayyip Erdoğan University (Rize, Turkey). All larva and honey samples were obtained from Bee Research Laboratories of Veterinary Control Institute (Samsun, Turkey). All isolates were grown on MYPG agar (Antunez et al. 2007; Dingman and Stahly 1983). The conventional methods including colony morphology examination, gram staining, physical and biochemical characterization were used to identify the strains. In addition, the molecular techniques such as partial sequence of 16S rRNA gene and American foulbrood-forward and American foulbrood-reverse specific primers for *P. larvae* were used to identify the isolates. The obtained 16S rRNA sequences were analyzed by BLAST searches using the NCBI GenBank database (Altschul et al. 1990; Benson et al. 2012; Dobbelaere et al. 2001). Finally, the sequences were used to construct phylogenetic tree to verify isolate identification (data were not shown).

The other group of the tested microorganisms were obtained from the Public Health Institution of Turkey and included the following microorganisms: *Escherichia coli* strain ATCC35218, *Yersinia pseudotuberculosis* strain ATCC911, *Pseudomonas aeruginosa* strain ATCC43288, *P. aeruginosa* strain ATCC 27853, *Enterococcus faecalis* strain ATCC29212, *Listeria monocytogenes* strain ATCC 43251, *Staphyloccus aureus* strain ATCC25923, *Bacillus cereus* strain 709 Roma, *B. subtilis* subs. *spizizenii* strain ATCC 6633, *Mycobacterium smegmatis* strain ATCC607, *Candida albicans* strain ATCC60193 and *Saccharomyces cerevisia* strain RSKK 251.

Antimicrobial activity assays

The agar well diffusion method was used to determine antimicrobial activity of the AgNPs (Ahmad et al. 1998). Each microorganism was suspended in a suitable medium to set it to 0.5-McFarland units turbidity. Then, the suspensions were spread on separate agar plates using sterile swabs. Five-millimeter diameter wells were cut the agar using a sterile cork-borer, and then the agar plates were dried. The wells were filled with 50 µl of AgNPs. *Paenibacillus*

strains were suspended in MYPG (10 g Mueller Hilton Broth, 15 g yeast extract, 1 g sodium pyruvate, 2 g glucose, 3 g K_2HPO_4) broth and spread on MYPG agar plates. *M. smegmatis* strain was suspended in BHI broth and spread on BHI agar plates. The yeast-like fungi were suspended in yeast extract broth and spread on PDA plates. All remaining microorganisms was suspended in MHB and spread on MHA plates. The plates were incubated at 35 °C for 18 h for bacteria and at 25 °C for 48 h for yeast. After the incubation, the antimicrobial activity was evaluated by measuring the zone of inhibition against the tested organisms. The inoculation plates were sealed with a parafilm to protect the water loss and contamination, and incubated at laboratory temperature for 1 month. The inhibition zone was measured with calipers on a weekly basis. Due to the absence of significant changes, the experiments were stopped after the fourth week. The second and fourth week results were taken into consideration for the evaluation.

The antimicrobial effect of the AgNPs was tested quantitatively in liquid broth media by using double microdilution, and the MIC values, as μg ml^{-1} were determined. The antibacterial assays were performed in MHB, MYPGP and BHI at pH 7.0, and antifungal assays were performed in buffered Yeast Nitrogen Base (YNB) at pH 7.0. The micro dilution test plates of MHB were incubated for 18–24 h at 35 °C. BHI, MYPGP and YNB broths were incubated for 48–72 h at 35 °C according to the literature (Singh et al. 2014).

Statistical analysis

Agar well diffusion and MIC results were statistically were analyzed using one-way ANOVA and when $P < 0.05$ were considered statistically significant.

Results

Synthesis and characterization of AgNPs

The AgNPs used in this study were synthesized with maltose reduction without using a stabilizer. The UV–Vis spectrum of pale yellow AgNPs colloidal suspension is shown in Fig. 1a. The spectrum exhibits an absorption maximum at 420 nm, which is typical surface plasmon resonance absorption band for spherical AgNPs. The dynamic light scattering spectrum provided in Fig. 1b indicates that the average hydrodynamic size of AgNPs is around 39 ± 15 nm. The UV–Vis spectrum and polydispersity index value (0.395 ± 0.054) suggest that the AgNPs have a very narrow size distribution profile. The transmission electron microscopy images on Fig. 1c and d show the actual size and morphology of the AgNPs. As seen, the AgNPs are mostly spherical in shape with about 20 nm sizes, relatively mono-disperse, and in the form of well-ordered single crystals.

Surface chemistry of AgNPs plays an important role for their action in biological media. Therefore, their surface chemistry was investigated with FTIR spectroscopy. Figure 2 shows the comparison of FTIR spectra obtained from maltose and the maltose reduced AgNPs. The broad peak observed at 3300 cm^{-1} is assigned to O–H stretching vibration of maltose (Mochochoko et al. 2013; Singh et al. 2014). The peaks at 2926 and 1079 cm^{-1} originate from C–H stretching of sp^3 carbon and typical stretching of O–C of maltose ring, respectively. The peak at ∼ 1710 cm^{-1} is assigned to vibrations of C=O (Kora et al. 2012; Mochochoko et al. 2013; Singh et al. 2014). The peaks at 1717 and 1643 cm^{-1} indicate the presence of an aldehyde or ketone functional group. These peaks indicate that the presence of maltose or maltose related molecules on the surface of AgNPs.

Antimicrobial effect of silver nanoparticles

The antimicrobial activity of AgNPs against the standard strains was evaluated using agar well diffusion and MIC methods (Table 1 and Fig. 3). The agar well diffusion results indicate that the AgNPs are very effective on *S. aureus* ATCC25923 and *M. smegmatis* ATCC607. The MIC value of the AgNPs against standard microorganisms was determined as 0.37 μg ml^{-1} except for *M. smegmatis.*

The antimicrobial activity of the AgNPs was also studied against 25 different spore forming bacteria (including *Bacillus, Paenibacillus* and *Micrococcus* strains) isolated from American foulbrood and European foulbrood suspicious samples (Table 2). Three of six different *P. larvae* strains, responsible for American foulbrood generated 13–20 mm inhibition zones and the zone diameters did not change during 4 weeks. However, the zone diameter of *P. larvae* strain PB 16.1b increased and zone diameters were measured as

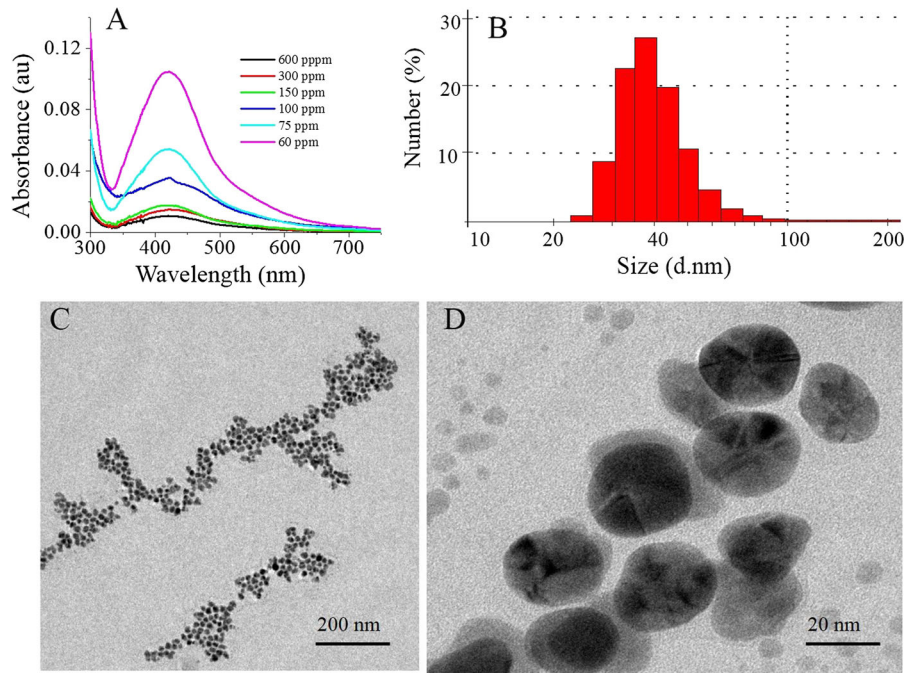

Fig. 1 UV/Vis absorption spectrum (**a**), dynamic light scattering spectrum (**b**), transmission electron microscopy images (**c**, **d**) of AgNPs

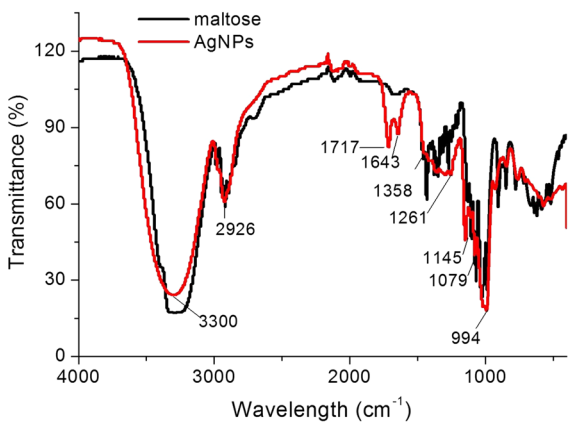

Fig. 2 Comparison of FTIR spectra of maltose and maltose reduced AgNPs

19 mm after the 4 weeks (Table 2). The one *P. alvei* strain causing European foulbrood generated 11 mm inhibition zone and the zone diameter did not change with the increasing time. The susceptibility of four saprophytic *Paenibacillus dendritiformis* strains against the maltose reduced AgNPs was also tested. From the results, PB 14a strain was not affected while PB18a and PB26a strains showed unchanged inhibition zones during 4 weeks. However, PB32a strain showed a time dependent inhibition zone. The fourteen different spore forming *Bacillus* and *Micrococcus* species including normal bacterial flora of *Apis mellifera* were also tested. The inhibition zone changes of these strains with time are provided in Table 2. For the tested strains, the MIC values were determined to be in the range of 3 to 12.5 μg ml^{-1}.

Discussion

There is a large number of AgNP synthesis methods reported in the literature using variety of reducing agents including plant extracts, and bacterial and fungal metabolites (Ahmad et al. 1998; Dingman and Stahly 1983; Dong et al. 2009; Mochochoko et al. 2013; Sharma et al. 2009; Tran et al. 2013; Vahabi et al. 2011). However, the resulting AgNP containing suspensions may or may not show antibacterial activity. This can be explained with the existence of two separate factor affecting AgNPs on microorganisms: size and dissolution rate. The smaller the size is the higher the antibacterial effect. The dissolution rate also strongly depends on synthesis method. When a strong reducing agent is used to prepare AgNPs, a tightly packed crystal lattice is formed. It is opposite when a weak reducing agent is used for the synthesis. The release of Ag^+ ions is faster from the latter. Carbohydrates are weak reducing agents for Ag^+ ions

Table 1 Agar well diffusion and MIC results of maltose reduced AgNPs against standard strains

Bacterial strain	Antibacterial Effect	
	Zone of inhibition (mm), (80 ppm, 50 μL AgNPs)	MIC value (μg/mL)[a]
Escherichia coli ATCC 25922	14.1 ± 0.1	0.37
Yersinia pseudotuberculosis ATCC 911	12.2 ± 0.2	0.37
Pseudomonas aeruginosa ATCC 43288	12.0 ± 0.1	0.37
Pseudomonas aeruginosa ATCC 27853	18.0 ± 0.1	0.37
Staphylococcus aureus ATCC 25923	25.5 ± 0.2	0.37
Enterococcus faecalis ATCC 13048	10.1 ± 0.1	0.37
Paenibacillus larvae LMG9820	14.2 ± 0.2	0.37
Bacillus cereus 702 Roma[b]	13.2 ± 0.2	0.37
B. subtilis subs. *spizizenii* ATCC 6633	9.0 ± 0.3	0.37
Mycobacterium smegmatis ATCC607	16.3 ± 0.2	2.0
Candida albicans ATCC 60193	8.1 ± 0.2	0.37
Saccaromyces cerevisiae RSKK 251	8.2 ± 0.1	0.37

[a]MIC STD less than 0.1 μg/ml

[b]Spore forming bacteria

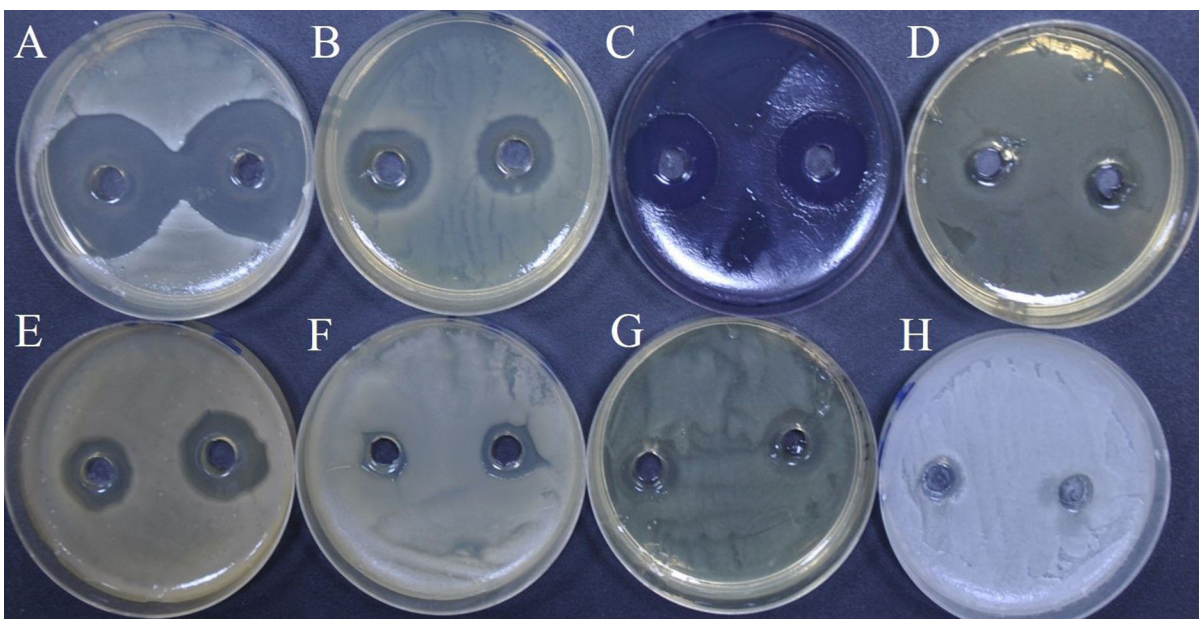

Fig. 3 Antibacterial activity of AgNPs against **a** *S. aureus*, **b** *E. coli*, **c** *P. aeruginosa*, **d** *Paenibacillus alvei PB34*, **e** *B. cereus*, **f** *B. subtilis subs. spizizenii*, **g** *P. larvae LMG9820*, **h** *C. albicans* strains. 80 μg/50 μL AgNPs were used in all experiments

forming loosely packed AgNP crystals, which are more prone to release of Ag^{+} ions in aqueous media. When this effect is combined with a size effect, such a colloidal suspension behaves as an effective antibacterial agent. For example, the reduction of Ag^{+} with tri-sodium citrate is a commonly used AgNP synthesis method (Lee and Meisel 1982). However, their biocidal effect is very low due to their large size (average 50 nm) and low dissolution rate.

Table 2 Antimicrobial activity of maltose reduced AgNPs against bacterial strains isolated from disease suspected larvae and honey samples

Bacterial strain	Number of strains (N: 31)	Zone of inhibition (mm)*		
		2 days	2 weeks	4 weeks
Bacillus sp.	2	–	14 ± 1	14 ± 1
B. subtilis	2	–	15 ± 3	15 ± 3
	3	6 ± 2	20 ± 5	20 ± 4
B. altitudinis	3	–	20 ± 2	20 ± 2
B. stratosphericus	1	–	15 ± 1	15 ± 1
B. pumilis	1	–	11 ± 1	11 ± 2
Paenibacillus larvae	1	–	–	–
	3	–	16 ± 4	20 ± 5
	2	13 ± 2	13 ± 2	13 ± 2
Paenibacillus alvei	1	–	10 ± 1	12 ± 1
Micrococcus kristinae	2	11 ± 1	11 ± 1	11 ± 1
P. dendritiformis	5	–	–	–
	2	12 ± 2	12 ± 2	12 ± 2
	3	5 ± 1	15 ± 5	25 ± 5
P. larvae LMG9828	1	12 ± 1	13 ± 1	16 ± 2

– no activity

*milimeter

The UV–Vis spectroscopy is a primary technique used for the characterization of AgNPs. The maximum absorption wavelength and its shift of surface plasmon resonance peak provides information about their size, dielectric medium and surface-adsorbed species (Pal et al. 2007). A shift of surface plasmon resonance to longer wavelengths means increased particle size (Pal et al. 2007). The hydrodynamic size of AgNPs is found to be 39 ± 15 nm but TEM images (Fig. 1c and d) show that the most of the AgNPs are around 23 nm. However, note that TEM image are representative in nature and does not provide a general picture of the size distribution but it provides morphological information. As seen from the TEM images, the AgNPs are spherical with a smooth topography. Note that the size of the particles is observed larger in aqueous medium due to the hydration layer in dynamic light scattering measurements (Jang et al. 2015). The zeta potential of the AgNPs was measured as −23.4 ± 2.7 mV indicating the presence of negatively charged ions and molecular species on the surface. The value of zeta potential gives important information about the stability of colloidal particles in their suspensions. The more negative zeta potential means higher stability for the particles. As zeta potential approaches zero, electrostatic repulsion forces between the colloidal particles decreases and eventually the particles stick together and precipitate (Greenwood and Kendall 1999; Hanaor et al. 2012). The zeta potential value of the maltose reduced AgNPs indicates that they are relatively stable.

During the oxidation–reduction reaction, the side products can also influence the surface chemistry, then thus aggregation properties of AgNPs, and the release of Ag^{+} ions from the surface. Therefore, the choice of reducing materials for synthesis is critical. The surface chemistry of AgNPs after the synthesis was investigated by using FTIR spectroscopy (Fig. 2). Observed vibrations indicate the presence of carbohydrates, possibly weakly bound degradation products of maltose on the AgNPs surface. The peak shifts observed at 3300, 1145, and 994 cm^{-1} suggest the binding of maltose or its degradation products to the AgNP surfaces through hydroxyl groups.

Antimicrobial activity of AgNPs against bacteria that were isolated from bee samples with American foulbrood and European foulbrood symptoms were investigated. The antimicrobial activity of AgNPs was also studied against a broad-spectrum of bacteria including highly pathogenic strains. The results of agar well diffusion and micro dilution tests indicate that AgNPs were very effective against all tested human pathogenic bacteria, fungi strains and pathogenic bacteria causing bee diseases (Tables 1 and 2). The most obvious effect was shown on the human pathogen, *M. smegmatis*. The spore-forming *P. larvae*

and *P. alvei* cause the death of bee colonies and spores survive for a long time in nature and contaminate bee species and bee products. Our results suggest that the AgNPs have a bacteriostatic and bactericidal effects against *Paenibacillus* sp. and they have the ability to inhibit spore formation at a lower dose (≤ 6 μg ml^{-1}). The antibiotics that used in bee diseases are to be effective, only infection periods and the infectious spores are not completely removed or killed. In addition residues of antibiotics were found in honey and bee equipment, which indicates the accumulation of antibiotics in time (Kora et al. 2012). The results of this study clearly suggests that maltose reduced AgNPs are a strong candidate for treatments of bee diseases as an alternative to antibiotics.

The mechanism of the antibacterial effect of AgNPs is mostly dependent on releasing of Ag^+ ions as stated before. As the particle size gets smaller, the antibacterial effect gets greater since the interaction between the bacteria cell wall and the AgNPs becomes more effective (Dobias and Bernier-Latmani 2013; Pal et al. 2007; Sharma et al. 2009). The interaction of AgNPs with about 21.2 nm diameters with bacterial cell wall results with the increased membrane permeability, which causes the death of bacteria (Morones et al. 2005). The inhibitory action of Ag^+ on bacterial cells is related to the affinity of Ag^+ with sulfur and phosphorus groups present in key respiratory enzymes in bacteria (Gordon et al. 2010). The dissolved Ag^+ can interact with DNA, resulting in inactivation of DNA replication, or can react with proteins, leading to the inhibition of enzyme functions. At the same time, metal ions can generate of intracellular reactive oxygen species in bacteria and the cell death (Stohs and Bagchi 1995).

Although the maltose reduced AgNPs used in this study are effective against the tested microorganisms, the question for the possible health effect upon their use on honeybees are not clear yet. There is a large number of studies regarding the possible adverse effects of AgNPs reported in the literature (Gonzalez et al. 2016; Kim et al. 2008; Raj et al. 2017; Shahare et al. 2013). In some of these studies, the AgNPs were found to toxic. For example, Gonzalez et al. found that AgNPs affect the epithelial cell microvilli as well as intestinal glands (Gonzalez et al. 2016). Kim et al. studied exposure of AgNPs on rats and found that the levels of hematocrit and hemoglobin after a 28-day oral exposure (Kim et al. 2008) increased. Raj et al. found that egg laying capability along with growth of ovary in adult insects were impaired with AgNP exposure (Raj et al. 2017). On the other hand, there are also studies suggesting that AgNPs may not cause significant harmful effects. For example, Tran et al. reported that AgNPs did not induce genetic toxicity in male and female rat bone marrow (Tran et al. 2013). The influence of size, shape, and surface chemistry on toxic effect of nanomaterials can help to explain the variations in the results of the reports. The dosage and dissolution rate of AgNPs are the other factors that can contribute the variation in results.

The minimum concentration of ions that can be tolerated by humans in drinking water is suggested as 100 ppm by WHO (Organization of Word Health, Guidelines for drinking-water quality 2011). Since the concentration of AgNPs used in this study is 80 ppm, it may be considered as safe to use the maltose reduced colloidal suspension of AgNPs for American and European foulbrood diseases. However, accumulation of AgNPs with long term use in the environment can cause adverse effects (Raj et al. 2017). In conclusion, the use of AgNPs is expected to provide a significant contribution and long-term efficacy because of the dissolution properties of AgNPs.

Acknowledgements We acknowledge the support from the Yeditepe University and Recep Tayyip Erdoğan University (Project No: 2015.53001.102.03.04).

Compliance with ethical standards

Conflict of interest All authors declare that there is no conflict of interest.

References

Agnihotri S, Mukherji S, Mukherji S (2014) Size-controlled silver nanoparticles synthesized over the range 5–100 nm using the same protocol and their antibacterial efficacy. RSC Adv 4:3974–3983. doi:10.1039/c3ra44507k

Ahmad I, Mehmood Z, Mohammad F (1998) Screening of some Indian medicinal plants for their antimicrobial properties. J Ethnopharmacol 62:183–193. doi:10.1016/S0378-8741(98)00055-5

Altschul SF, Gish W, Miller W, Myers EW, Lipman DJ (1990) Basic local alignment search tool. J Mol Biol 215(3):403–410. doi:10.1016/S0022-2836(05)80360-2

Ansari MA, Khan HM, Khan AA, Cameotra SS, Alzohairy MA (2015) Anti-biofilm efficacy of silver nanoparticles against MRSA and MRSE isolated from wounds in a tertiary care

hospital. Indian J Med Microbiol 33:101–109. doi:10.4103/0255-0857.148402

Antunez K, Piccini C, Castro-Sowinski S, Rosado AS, Seldin L, Zunino P (2007) Phenotypic and genotypic characterization of *Paenibacillus larvae* isolates. Vet Microbiol 124:178–183. doi:10.1016/j.vetmic.2007.04.012

Benson DA, Karsch-Mizrachi I, Clark K, Lipman DJ, Ostell J, Sayers EW (2012) GenBank. Nucleic Acids Res 40:D48–D53. doi:10.1093/nar/gkr1202

Besinis A, De Peralta T, Handy RD (2014) The antibacterial effects of silver, titanium dioxide and silica dioxide nanoparticles compared to the dental disinfectant chlorhexidine on *Streptococcus mutans* using a suite of bioassays. Nanotoxicology 8:1–16. doi:10.3109/17435390.2012.742935

Biswas A, Bayer IS, Biris AS, Wang T, Dervishi E, Faupel F (2012) Advances in top-down and bottom-up surface nanofabrication: techniques, applications & future prospects. Adv Colloid Interface Sci 170:2–27. doi:10.1016/j.cis.2011.11.001

Brust M, Kiely CJ (2002) Some recent advances in nanostructure preparation from gold and silver particles: a short topical review. Colloids Surf A 202:175–186

Chauzat M-P, Laddomada A (2015) The Coloss Beebook Volume II—Foreword. J Apic Res 52:1–2. doi:10.3896/ibra.1.52.4.17

Dingman DW, Stahly DP (1983) Medium promoting sporulation of *Bacillus larvae* and metabolism of medium components. Appl Environ Microbiol 46:860–869

Dobbelaere W, de Graaf DC, Peeters JE (2001) Development of a fast and reliable diagnostic method for American foulbrood disease (*Paenibacillus larvae* subsp. *larvae*) using a 16S rRNA gene based PCR. Apidologie 32:363–370. doi:10.1051/apido:2001136

Dobias J, Bernier-Latmani R (2013) Silver release from silver nanoparticles in natural waters. Environ Sci Technol 47:4140–4146. doi:10.1021/es304023p

Dong X, Ji X, Wu H, Zhao L, Li J, Yang W (2009) Shape control of silver nanoparticles by stepwise citrate reduction. J Phys Chem C 113:6573–6576. doi:10.1021/jp900775b

Dubas ST, Kumlangdudsana P, Potiyaraj P (2006) Layer-by-layer deposition of antimicrobial silver nanoparticles on textile fibers. Colloids Surf A 289:105–109. doi:10.1016/j.colsurfa.2006.04.012

Frey NA, Peng S, Cheng K, Sun S (2009) Magnetic nanoparticles: synthesis, functionalization, and applications in bioimaging and magnetic energy storage. Chem Soc Rev 38:2532–2542. doi:10.1039/b815548h

Genersch E (2010) American Foulbrood in honeybees and its causative agent, *Paenibacillus larvae*. J Invertebr Pathol 103(Suppl 1):S10–S19. doi:10.1016/j.jip.2009.06.015

Gonzalez C, Rosas-Hernandez H, Ramirez-Lee MA, Salazar-García S, Ali SF (2016) Role of silver nanoparticles (AgNPs) on the cardiovascular system. Arch Toxicol 90:493–511. doi:10.1007/s00204-014-1447-8

Gordon O, Vig Slenters T, Brunetto PS, Villaruz AE, Sturdevant DE, Otto M, Landmann R, Fromm KM (2010) Silver coordination polymers for prevention of implant infection: thiol interaction, impact on respiratory chain enzymes, and hydroxyl radical induction. Antimicrob Agents Chemother 54:4208–4218. doi:10.1128/AAC.01830-09

Greenwood R, Kendall K (1999) Selection of suitable dispersants for aqueous suspensions of zirconia and titania powders using acoustophoresis. J Eur Ceram Soc 19:479–488

Haider A, Kang I-K (2015) Preparation of silver nanoparticles and their industrial and biomedical applications: a comprehensive review. Adv Mater Sci Eng 2015:1–16. doi:10.1155/2015/165257

Hanaor D, Michelazzi M, Leonelli C, Sorrell CC (2012) The effects of carboxylic acids on the aqueous dispersion and electrophoretic deposition of ZrO 2. J Eur Ceram Soc 32:235–244

Jang M-H, Lee S, Hwang YS (2015) Characterization of silver nanoparticles under environmentally relevant conditions using asymmetrical flow field-flow fractionation (AF4). PLoS ONE 10:e0143149. doi:10.1371/journal.pone.0143149

Kim YS, Kim JS, Cho HS, Rha DS, Kim JM, Park JD, Choi BS, Lim R, Chang HK, Chung YH, Kwon IH, Jeong J, Han BS, Yu IJ (2008) Twenty-eight-day oral toxicity, genotoxicity, and gender-related tissue distribution of silver nanoparticles in Sprague-Dawley rats. Inhal Toxicol 20:575–583. doi:10.1080/08958370701874663

Kong H, Jang J (2008) Antibacterial properties of novel poly(-methyl methacrylate) nanofiber containing silver nanoparticles. Langmuir 24:2051–2056. doi:10.1021/la703085e

Kora AJ, Beedu SR, Jayaraman A (2012) Size-controlled green synthesis of silver nanoparticles mediated by gum ghatti (*Anogeissus latifolia*) and its biological activity. Org Med Chem Lett. doi:10.1186/2191-2858-2-17

Lee PC, Meisel D (1982) Adsorption and surface-enhanced Raman of dyes on silver and gold sols. J Phys Chem C 86:3391–3395. doi:10.1021/j100214a025

Llror C, Bjerrum L (2014) Antimicrobial resistance: risk associated with antibiotic overuse and initiatives to reduce the problem. Ther Adv Drug Saf 5:229–241. doi:10.1177/2042098614554919

Mochochoko T, Oluwafemi OS, Jumbam DN, Songca SP (2013) Green synthesis of silver nanoparticles using cellulose extracted from an aquatic weed; water hyacinth. Carbohydr Polym 98:290–294. doi:10.1016/j.carbpol.2013.05.038

Morones JR, Elechiguerra JL, Camacho A, Holt K, Kouri JB, Ramirez JT, Yacaman MJ (2005) The bactericidal effect of silver nanoparticles. Nanotechnology 16:2346–2353. doi:10.1088/0957-4484/16/10/059

OIE World Organisation of Animal Health. Manual of diagnostic tests and vaccines for terrestrial animals 2017. Alippi, A. Chapter 2.2.2. American foulbrood of honey bees (infection of honey bees with Paenibacillus larvae) (NB: Version adopted in May 2016). pp 1–17

Organization of Word Health (2011) Guidelines for drinking-water quality. World Health Organization, Geneva

Özkırım A, Çelemli ÖG, Schiesser A, Charistos L, Hatjina F (2015) A comparison of the activities of Greek and Turkish propolis against *Paenibacillus larvae*. J Apic Res 53:528–536. doi:10.3896/ibra.1.53.5.01

Pal S, Tak YK, Song JM (2007) Does the antibacterial activity of silver nanoparticles depend on the shape of the nanoparticle? A study of the Gram-negative bacterium *Escherichia*

coli. Appl Environ Microbiol 73:1712–1720. doi:10.1128/AEM.02218-06

Petros RA, DeSimone JM (2010) Strategies in the design of nanoparticles for therapeutic applications. Nat Rev Drug Discov 9:615–627. doi:10.1038/nrd2591

Raj A, Shah P, Agrawal N (2017) Dose-dependent effect of silver nanoparticles (AgNPs) on fertility and survival of Drosophila: an in vivo study. PLoS ONE 12:e0178051. doi:10.1371/journal.pone.0178051

Raveendran P, Fu J, Wallen SL (2003) Completely "green" synthesis and stabilization of metal nanoparticles. J Am Chem Soc 125:13940–13941

Reybroeck W, Daeseleire E, De Brabander HF, Herman L (2012) Antimicrobials in beekeeping. Vet Microbiol 158:1–11. doi:10.1016/j.vetmic.2012.01.012

Shahare B, Yashpal M, Gajendra (2013) Toxic effects of repeated oral exposure of silver nanoparticles on small intestine mucosa of mice. Toxicol Mech Methods 23:161–167. doi:10.3109/15376516.2013.764950

Sharma VK, Yngard RA, Lin Y (2009) Silver nanoparticles: green synthesis and their antimicrobial activities. Adv Colloid Interface Sci 145:83–96. doi:10.1016/j.cis.2008.09.002

Singh S, Bharti A, Meena VK (2014) Structural, thermal, zeta potential and electrical properties of disaccharide reduced silver nanoparticles. J Mater Sci 25:3747–3752. doi:10.1007/s10854-014-2085-x

Stohs SJ, Bagchi D (1995) Oxidative mechanisms in the toxicity of metal ions. Free Radic Biol Med 18:15. doi:10.1016/0891-5849(94)00159-H

Tran QH, Nguyen VQ, Le A-T (2013) Silver nanoparticles: synthesis, properties, toxicology, applications and perspectives. Adv Nat Sci 4:033001. doi:10.1088/2043-6262/4/3/033001

Tugulea AM, Berube D, Giddings M, Lemieux F, Hnatiw J, Priem J, Avramescu ML (2014) Nano-silver in drinking water and drinking water sources: stability and influences on disinfection by-product formation. Environ Sci Pollut Res Int 21:11823–11831. doi:10.1007/s11356-014-2508-5

Vahabi K, Mansoori GA, Karimi S (2011) Biosynthesis of silver nanoparticles by fungus *Trichoderma reesei* (a route for large-scale production of AgNPs). Insciences J 1(1):65–79. doi:10.5640/insc.010165

Wilson WT (1971) Resistance to American foulbrood in honey bees. J Invertebr Pathol 17:247–255